

#### **OPEN ACCESS**

EDITED BY Luigi Dell'Olio, University of Cantabria, Spain

REVIEWED BY
Yanyan Qin,
Chongqing Jiaotong University, China
Luca Mantecchini,
University of Bologna, Italy
Rajanish Kumar Kaushal,
Chandigarh University, India

\*CORRESPONDENCE
Davoud Alahvirdi,

davoud.alahvirdi@unamur.be

RECEIVED 09 July 2025 ACCEPTED 21 August 2025 PUBLISHED 05 September 2025

#### CITATION

Alahvirdi D and Tuci E (2025) Traffic monitoring and management system based on a swarm of drones and adaptive traffic units. Front. Future Transp. 6:1662822. doi: 10.3389/ffutr.2025.1662822

#### COPYRIGHT

© 2025 Alahvirdi and Tuci. This is an openaccess article distributed under the terms of the Creative Commons Attribution License (CC BY). The use, distribution or reproduction in other forums is permitted, provided the original author(s) and the copyright owner(s) are credited and that the original publication in this journal is cited, in accordance with accepted academic practice. No use, distribution or reproduction is permitted which does not comply with these terms.

# Traffic monitoring and management system based on a swarm of drones and adaptive traffic units

Davoud Alahvirdi\* and Elio Tuci

Robotics Lab, Computer Science Faculty, University of Namur, Namur, Belgium

Traffic monitoring is a critical aspect of urban infrastructure management. With the advancement of technologies, traditional surveillance methods based on fixed sensor network systems could be potentially replaced by adaptive and easily redeployable systems, such as those based on drones. This paper wishes to contribute to the development of drones-based traffic monitoring and management systems by describing and evaluating a simulated swarm of drones monitoring traffic and communicating traffic data to adaptive traffic lights which adapt their green light duration to the current volume of traffic using the SPSA optimisation algorithm. A cell transition model (CTM) is used to simulate the behaviour, flow, and interactions of vehicles within a road network larger than most of networks used in similar studies. Evaluation tests compare the effectiveness of adaptive traffic unit with data generated by drones with a system of fixed duration signal traffic lights, and with an adaptive traffic unit with data generated by fixed cameras. The results shows that the optimised traffic lights system with data generated by drones is more effective than both the fixed signalling duration and the optimised system with data generated by fixed cameras in resolving traffic congestion due to a high volume of cars entering the road network. Further post-evaluation tests illustrate the limits of the adaptive traffic unit system with data generated by drones under a progressively higher volume of traffic entering the road network. We conclude the paper by discussing the current limitations of our model and by pointing to the most interesting directions for future work.

KEYWORDS

smart city, traffic monitoring and management, cell transition model, adaptive traffic unit, route planning, simultaneous perturbation stochastic approximation

## 1 Introduction

Unmanned aerial vehicles (UAVs), commonly known as drones, have emerged as a transformative force in various fields such as precision agriculture, wildlife conservation, delivery, logistics, and etc. The ability for vertical take-off and landing within limited spaces and their impressive speed and agility have induced researchers to exploit drones in a wide range of tasks in particular in those requiring surveillance and data collection such as traffic monitoring and management tasks. The exponential rise in the number of vehicles in the road networks have largely contributed to the emergence of frequent traffic congestion problems as well as of problems related to air and sound pollution in urban areas (Anjum et al., 2021; Goetz, 2019). Sensor-network based technology, exploiting fixed camera Radivojević et al. (2021), ultrasonic sensors Tan et al. (2020), and RFID—Radio Frequency Identification—reader Atta

et al. (2020), have made possible to address the negative effects of traffic on quality of life and on wellbeing of citizens with effective strategies to monitor, and possibly alleviate, vehicle congestion on urban roads and motorways (Fadda et al., 2022; Appiah et al., 2020; Tasgaonkar et al., 2020). For example, in Neelakandan et al. (2021); Zhang et al. (2020); Kuang et al. (2021); Desmira et al. (2022), a combination of fixed sensor-networks and different AI-based algorithms are presented to manage traffic by regulating trafficlight timing. These systems has been proved quite effective in reducing the average waiting time of vehicles in the road networks. Nevertheless, sensor-network based technology suffers from several limitations, primarily determined by the relatively high cost of maintenance operations such as sensor calibration, as well as from the fact that the technology is not particularly suitable to be deployed in very large areas (Narisetty et al., 2021; Ravish and Swamy, 2021). Furthermore, this technology, being anchored to the ground, completely lacks the flexibility and adaptability required to be easily and continuously redeployed in different areas to track the development of vehicle traffic on large road networks. To overcome the limitations of fixed sensor-networks, drones have emerged as a costs effective technology, that has the advantage to be easily deployed in different and potentially large urban zones to carry out tasks related to road safety, motorway infrastructure management, and traffic monitoring (Gohari et al., 2022; Dilshad et al., 2020; Bisio et al., 2022).

The scientific literature on single or multiple UAVs systems employed for urban activities, including traffic monitoring, is already quite vast. A possible way to sort this large body of research is by classifying these works in those that we referred to as "general" and those that we referred to as "specific." In the "general" category we include those research works that focus on challenges in urban air mobility common to multiple applications. Many of these studies focus on problem related to the generation of trajectories for UAVs required to fly at low altitudes in cluttered scenarios, characterised by natural and man-made obstacles. In Causa and Fasano (2021), the authors illustrate a obstacle-free path planning algorithm for multi UAVs based on the multi-step strategies that include automated definition of GNSS-challenging volumes based on a georeferenced three-dimensional environment model, derivation of candidate obstacle-free paths between waypoints, waypoint assignment and definition of time-tagged trajectories to cope with path planning issues in low altitude environment. In Nguyen et al. (2021), the authors developed a drones-based traffic monitoring system in which the drones fly on trajectories that are defined using GPS points. The scientific contribution of this work is in demonstrating that GPS trajectories are more effective than map based routes. In Elloumi et al. (2018), an innovative road traffic monitoring system is characterised by multiple drones generating adaptive flying trajectories, which are based on the tracking of moving points within the UAV field of view. Other papers propose algorithms that allow drones to minimise travel time in missions that require drones to visit multiple sites. For example, in Christodoulou and Kolios (2020) and Garcia-Aunon et al. (2019), the authors describe methods to allow drones to minimise travel time based on point of interests (POIs) and genetic algorithm, respectively.

In the "specific" category, we include those research works that focus on issues related to specific applications, with a main focus on research works in which air mobility is applied to the development of traffic monitoring and management systems. In Roldán-Gómez et al. (2022), a swarm of simulated drones is deployed to monitor traffic by counting the number of vehicles in a virtual city called swarm city and to share this data with a ground station unit. In these investigations, the shared data were used to generate maps represented in a virtual reality interface. In Hanzla et al. (2024), the authors introduce a smart traffic monitoring solution to address challenges in vehicle detection and tracking, by segmenting images taken by drones using deep learning technology (i.e., YOLOv5) and Kalman Filter based algorithms. In Zhu et al. (2018), the authors also exploited deep neural network algorithms to process videos recorded by a swarm of drones in order to detect and localise vehicles. Several drones-based traffic monitoring systems used a centralised approach in which the information gathered by drones is transferred to a human-operated central unit that processes the data and makes decisions concerning the management of traffic congestion. In studies that adopt this approach, the research focuses on issues related to the communication between drones and the central decision unit (Elloumi et al., 2018). Human errors, delays in response time, and difficulty in handling emergency conditions are the main drawbacks of the centralised traffic management systems (Yadav et al., 2021). To overcome these challenges, decentralised and adaptive traffic stations, exploiting machine learning methods (such as reinforcement learning algorithms), have been investigated. Some of these decentralised traffic systems regulate the traffic light duration as in Saleem et al. (2022); Abdoos and Bazzan (2021). In Chow et al. (2020), centralised and decentralised optimal control strategies are compared based on the Hamilton-Jacobi formulation of the kinematic traffic model. The optimal methodologies are applied to a set of test scenarios constructed from a real road network in central London (UK). In Yao et al. (2022), the authors illustrate an optimised traffic signal controller based on SPSA algorithm for a mixed traffic flow composed of automated and human driven vehicles by using CTM traffic model. The optimised control effectively reduces the range and the dissipation time of traffic congestion in comparison with fixed timing control. Mixed traffic flow is characterized by connected automated vehicles (CAVs), connected vehicles (CVs), and regular vehicles (RVs). In Qin et al. (2024), an analyticalmixed traffic capacity model for minor roads in an intersection is proposed to estimates their passing probabilities between CAV-led and CV/ RV-led platoons.

In most of the applications within the framework of urban air mobility, an advanced and reliable communication protocols is required to exchange data between drones and ground stations. Due to the limited resources available to run highly secure algorithms on board, authors in Hassija et al. (2021) investigated the effectiveness of communication methods such as blockchain, software defined networks (SDN), and machine learning to neutralise the effects of attacks such as man-in-the-middle or deauthentication. In Ivancic et al. (2019) and Guirado et al. (2021), the authors present internet-based communication protocols named 4G LTE method for real-time transfer of video and images between air traffic management units and small unmanned air vehicles to address communication challenges. In Aloqaily et al. (2022), a UAV-supported vehicular network is implemented where drones and traffic units are considered as separate nodes that communicate with each other through the 5G connection and ad hoc links. To

make communication more secure against cybersecurity attacks, a novel distributed way for drone-to-drone communication is illustrated in (Kumar et al., 2022). This secure method comes with some drawbacks such as limited bandwidth, spectrum constraints, and the requirement of the use of a large quantity of drones to cover a vast city map.

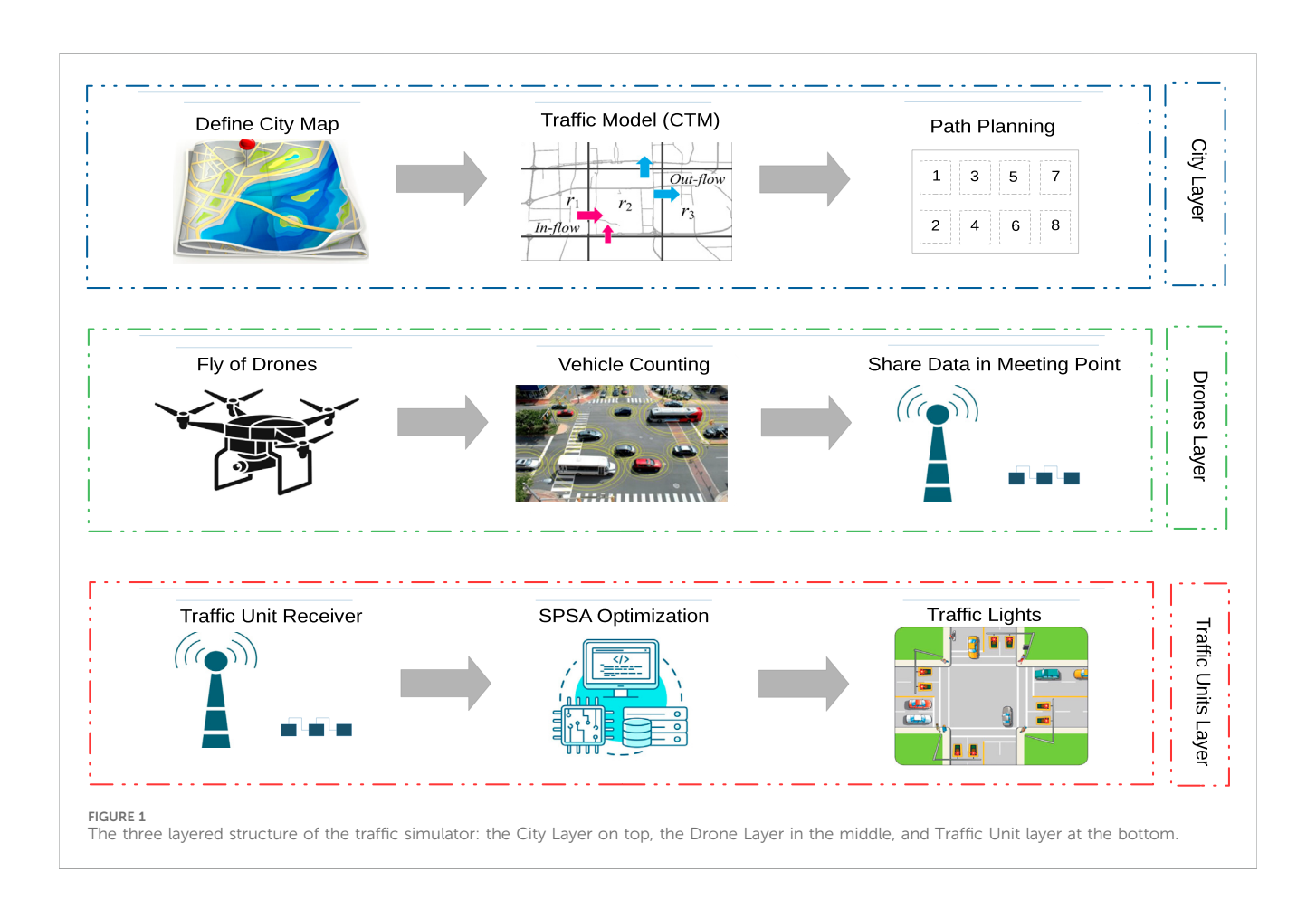
As in Yao et al. (2022) mentioned above, the research work described in this paper focuses on a system that manages traffic using drones. In particular, we illustrate and evaluate a decentralised multiple UAVs based system that by patrolling urban network, count cars on different roads and communicate this information to traffic lights signals. The signalling system uses this information to adjust signalling time using an optimisation method in order to reduce any eventual congestion. We consider a road network that consists of three connected two-way two-lanes cross intersections, we model traffic using CTM traffic model, and we defined fixed meeting points where the drones can share data with traffic light signals at regular intervals. We show that, when a high concentration of traffic is detected by drones in any part of the network, the traffic light unit concerned with the congestion, made aware of the problem by drones, resolves the congestion (i.e., it reduces the volume of traffic) by using the optimisation algorithm to adjust the green traffic light duration. In order to provide a term of comparison for the performance of the drones-based system, we also evaluate in identical conditions an alternative sensor-network based system in which information about traffic is generated and transferred to traffic lights by fixed camera. The results show that the drones-based

system is more effective than the sensor-network based system. The original contribution of this study is in demonstrating the effectiveness of the above described drones-based traffic management system in a more complex scenario than the one employed in other similar studies such as in (Yao et al., 2022). We target a more extended road network than those described in the literature for similar drone-based technology, with a greater number of interconnected intersections and a realistic traffic signalling system, where traffic units control and optimise the flow of forward/right turn, and left turn traffic. Moreover, we evaluate the robustness of the mentioned traffic management system in a larger set of traffic flow input conditions in comparison with (Yao et al., 2022).

The remaining of this paper is structured as follows: the general methodological approach is described in Section 2, with Section 2.1 and 2.2 illustrating the whole of the city layout model and the traffic light phases, respectively; Section 2.3 illustrating the traffic model; the route planning for the navigation of drones is described in Section 2.4; the traffic lights optimisation algorithm is illustrated in Section 2.5. Simulation results are shown in Section 3, and finally conclusions are drawn in Section 4.

## 2 Methodology

This Section describes the methods used to develop the simulation modelling an urban scenario with a swarm of drones



carrying out the traffic monitoring and management task. As illustrated in Figure 1, the simulation model is made of the following three layers: i) the city-layer, ii) the drone-layer, and iii) the traffic-layer. The city-layer includes the road map, the traffic model, and the routes the drones follow during inspection. The road map describes an urban environment, with a geographically realistic representation of road networks with lanes, intersection geometries, and relevant infrastructure such as traffic signals. The traffic is implemented using CTM which is an inflow-outflow mathematical formulation used to simulate and analyse the flow of traffic within the road network. The routes refer to the trajectories that drones follow to monitor the traffic. Each drone has two possible routes. The switching between routes by drones is triggered by specific conditions concerning the level of traffic within the route currently monitored. Within each route, there are meeting points; that is, points in which drones and traffic signals are sufficiently close (< 5 m) to be able to transmit each other data concerning the status of traffic while avoiding communication issues related to limited bandwidth. The dronelayer takes care of flying the drones along their trajectories while monitoring the traffic (i.e., by counting vehicles on the each of the road cells traversed during the flight). This layer also takes care of the communication between drones and traffic lights. As detailed later, the dynamic propagation process of traffic flow is discretised. Consequently, the drones also move in a discrete way between adjacent road cells at a given velocity. While above a road cell, each drone records the number of vehicles on that cell, as modelled by CTM. Anytime a drone reaches a meeting point, it transfers fresh data on traffic to the corresponding traffic signal. The traffic-layer runs the SPSA algorithm. This is an optimisation algorithm that uses the most recently available data on traffic to set the light signal cycle

in order to minimise the traffic on the cells of the entire road network. The traffic-layer also informs the drones to switch route anytime specific conditions on traffic are fulfilled. In the following, we describe in details the properties of the main components of this three-layers simulation model.

### 2.1 The road network

The road network is made of three two-way two-lanes cross intersections (four legs) connected as illustrated in Figure 2. Each leg has two entry and two exit points to the intersection. The entry points are one for vehicles moving forward and turning right, and the other entry for vehicles turning left. The exit points are one for receiving vehicles travelling forward and for those leaving the intersection with a right turn, and the other exit for vehicles leaving the intersection with a left turn. In the road network, there are a total of 48 entry/exit points to intersections, which we refer to as  $R_{\{i,j,k\}}$ , where  $i = \{1,2,3\}$  refers to the intersection number;  $j = \{IN_{fr}, IN_l, OUT_{fr}, OUT_l, \}$  refers to the lanes of each leg, with  $IN_{fr}$  for the vehicles entering the intersection to move forward and to turn right,  $IN_l$  for the vehicles entering the intersection to turn left,  $OUT_{fr}$  for the vehicles leaving the intersection with a forward movement and with a right turn,  $OUT_l$  for the vehicles leaving the intersection with a left turn; k = $\{W, E, N, S\}$  indicate the four legs of each intersection using the cardinal points. Similarly, we use  $L_{\{i,j,k\}}$  to denote the total length of the lanes. The traffic flows according to the Right-Hand Traffic (RHT) system. It follows that, for example, vehicles leaving intersection 1 from point  $R_{\{1,OUT_{fr},E\}}$ , enter into intersection 2 at point  $R_{\{2,IN_{fr},W\}}$ , while moving forward. Conversely, vehicles leaving

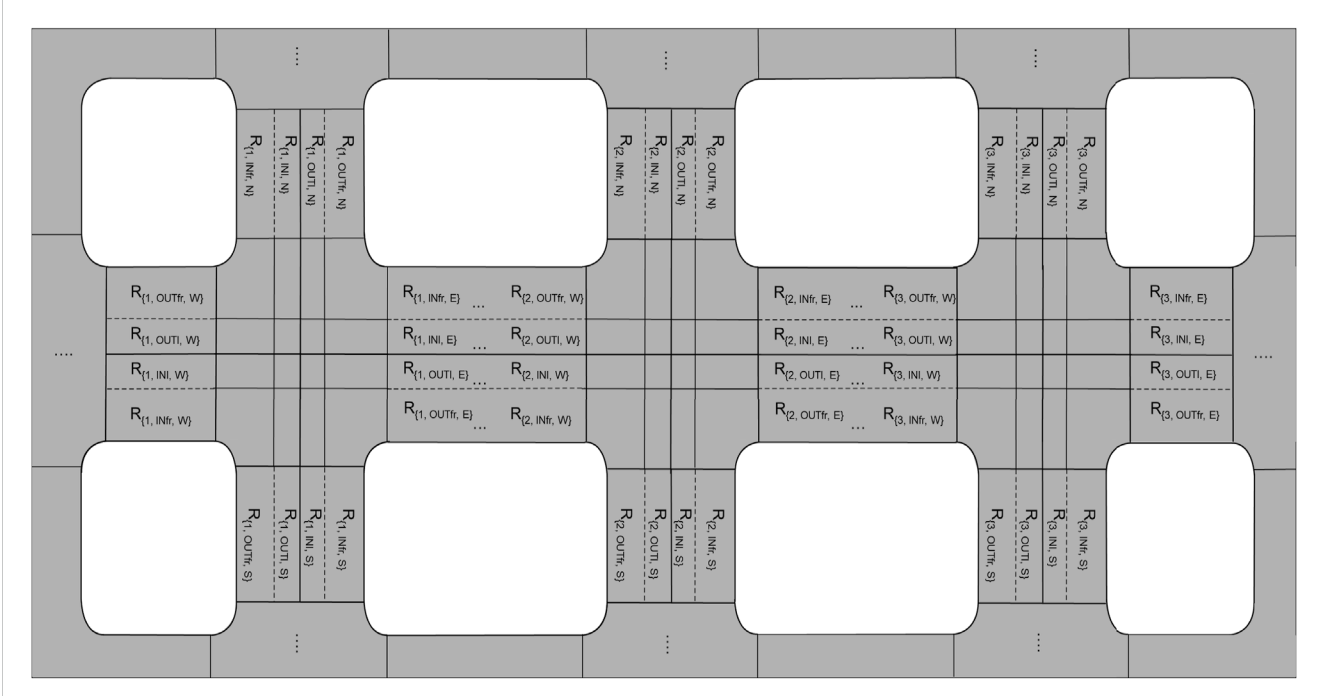
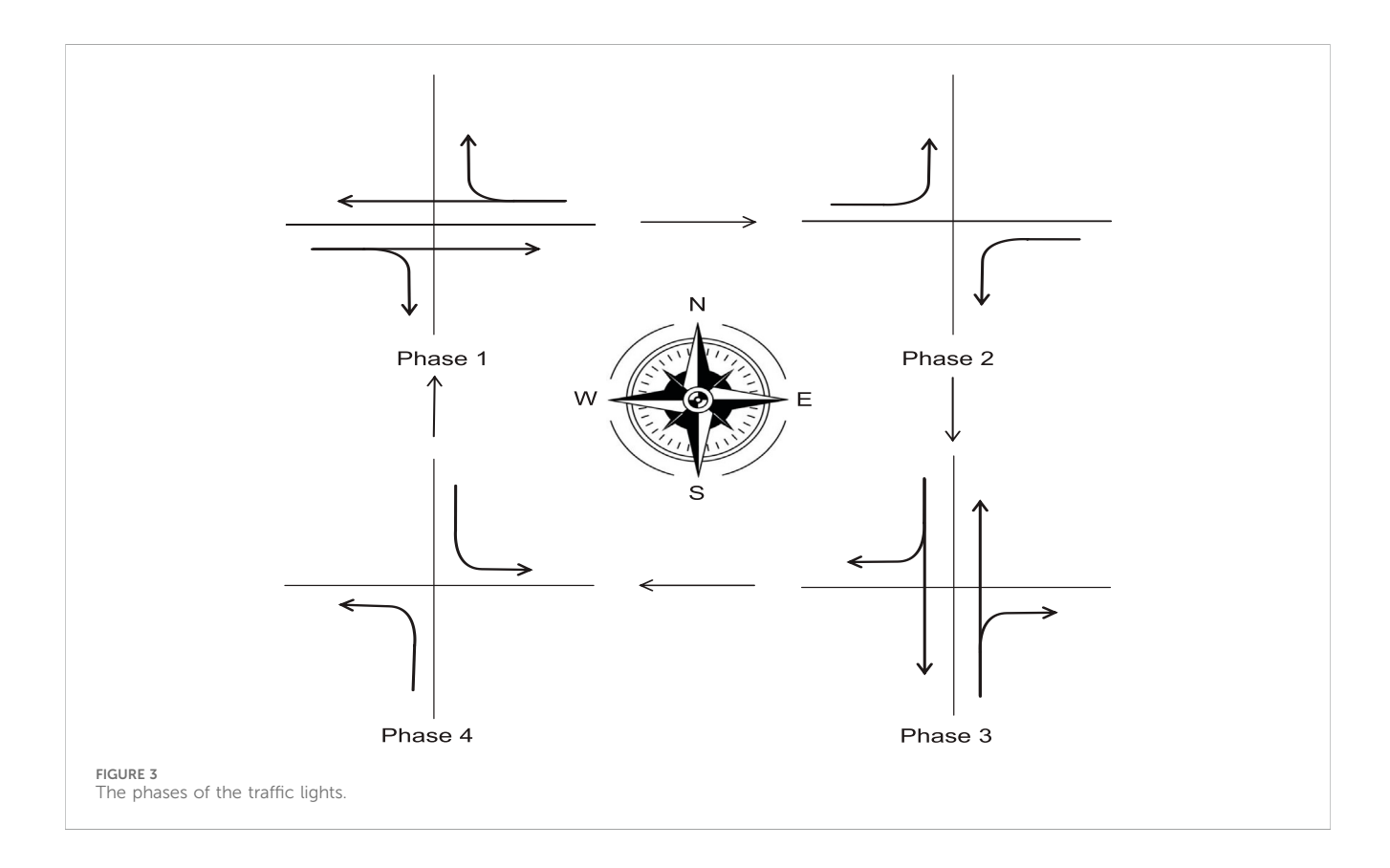


FIGURE 2
The road network made of three two-way two-lanes cross intersections. The notation refers to the entry and exit points to the intersections.



intersection 2 from point  $R_{\{2,OUT_{fr},W\}}$ , enter into intersection 1 at point  $R_{\{1,IN_{fr},E\}}$ , while moving forward.

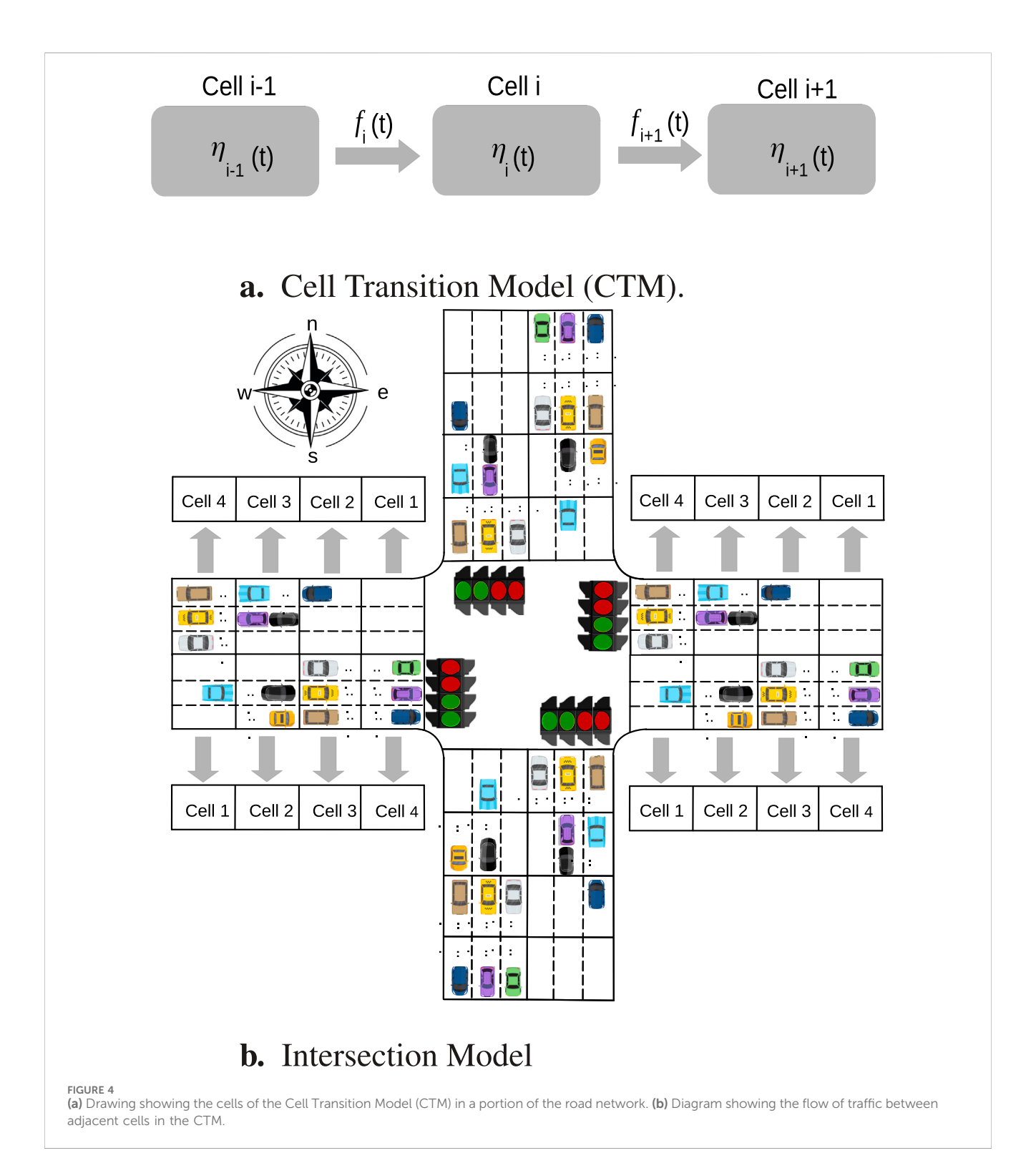
## 2.2 The three sets of traffic lights

Three sets of traffic signals control the traffic at each intersection. Each traffic light has a cycle characterised by four phases, as illustrated in Figure 3. In order to implement the four phases, each set is made of four traffic signals, with each traffic signal made of two subsets of two lights (i.e., one red and one green light). The two-light subset referred to as  $S_{\{i,IN_{fr},k,c\}}$ , with  $c = \{red, green\}$ , controls the movement of vehicles entering into intersection i from point  $R_{\{i,IN_{fr},k\}}$ , while the two-light subset referred to as  $S_{\{i,IN_{f},k,c\}}$ , controls the movement of vehicles entering into intersection i from point  $R_{\{i,IN_{fr},k\}}$ . For each set of traffic signals, the light cycle is characterised by the following four phases:

- phase 1: during this phase, the traffic at intersection *i* flows from the *W* to the *E* leg, and from the *E* to the *W* leg, for moving forward vehicles. Moreover, the traffic flows from the *W* to the *S* leg, and from the *E* to the *N* leg, for turning-right vehicles. This means that, in the *W* leg  $S_{\{i,IN_f,W,green\}}$ , and  $S_{\{i,IN_l,W,red\}}$ , while in the *E* leg and  $S_{\{i,IN_f,E,green\}}$ , and  $S_{\{i,IN_f,E,red\}}$ . All the other subsets have red lights; in the *N* leg  $S_{\{i,IN_f,N,red\}}$ ,  $S_{\{i,IN_l,N,red\}}$ , and in the *S* leg  $S_{\{i,IN_f,S,red\}}$ ,  $S_{\{i,IN_f,S,red\}}$ ,  $S_{\{i,IN_f,S,red\}}$ , and in the *S* leg  $S_{\{i,IN_f,S,red\}}$ ,  $S_{\{i,IN_f,S,red\}}$ ,  $S_{\{i,IN_f,S,red\}}$ .
- phase 2: during this phase, the traffic at intersection i flows from the W to the N leg, and from the E to the S leg, for

- turning-left vehicles. This means that, in the W leg  $S_{\{i,IN_{fr},W,red\}}$ , and  $S_{\{i,IN_{l},W,green\}}$ , while in the E leg and  $S_{\{i,IN_{fr},E,red\}}$ , and  $S_{\{i,IN_{l},E,green\}}$ . All the other subsets have red lights; in the N leg  $S_{\{i,IN_{fr},N,red\}}$ ,  $S_{\{i,IN_{l},N,red\}}$ , and in the S leg  $S_{\{i,IN_{fr},S,red\}}$ ,  $S_{\{i,IN_{l},S,red\}}$ .
- phase 3: during this phase, the traffic at intersection *i* flows from the *N* to the *S* leg, and from the *S* to the *N* leg, for moving forward vehicles. Moreover, the traffic flows from the *N* to the *W* leg, and from the *S* to the *E* leg, for turning-right vehicles. This means that, in the *N* leg  $S_{\{i,IN_f,N,green\}}$ , and  $S_{\{i,IN_f,N,red\}}$ , while in the *S* leg and  $S_{\{i,IN_f,S,green\}}$ , and  $S_{\{i,IN_f,S,red\}}$ . All the other subsets have red lights; in the *W* leg  $S_{\{i,IN_f,w,red\}}$ ,  $S_{\{i,IN_i,E,red\}}$ , and in the *E* leg  $S_{\{i,IN_f,E,red\}}$ ,  $S_{\{i,IN_i,E,red\}}$ .
- phase 4: during this phase, the traffic at intersection i flows from the N to the E leg, and from the S to the W leg, for turning-right vehicles. This means that, in the N leg  $S_{\{i,IN_f,N,red\}}$ , and  $S_{\{i,IN_i,N,green\}}$ , while in the S leg and  $S_{\{i,IN_f,S,red\}}$ , and  $S_{\{i,IN_f,S,green\}}$ . All the other subsets have red lights; in the W leg  $S_{\{i,IN_f,W,red\}}$ ,  $S_{\{i,IN_i,W,red\}}$ , and in the E leg  $S_{\{i,IN_f,E,red\}}$ ,  $S_{\{i,IN_i,E,red\}}$ .

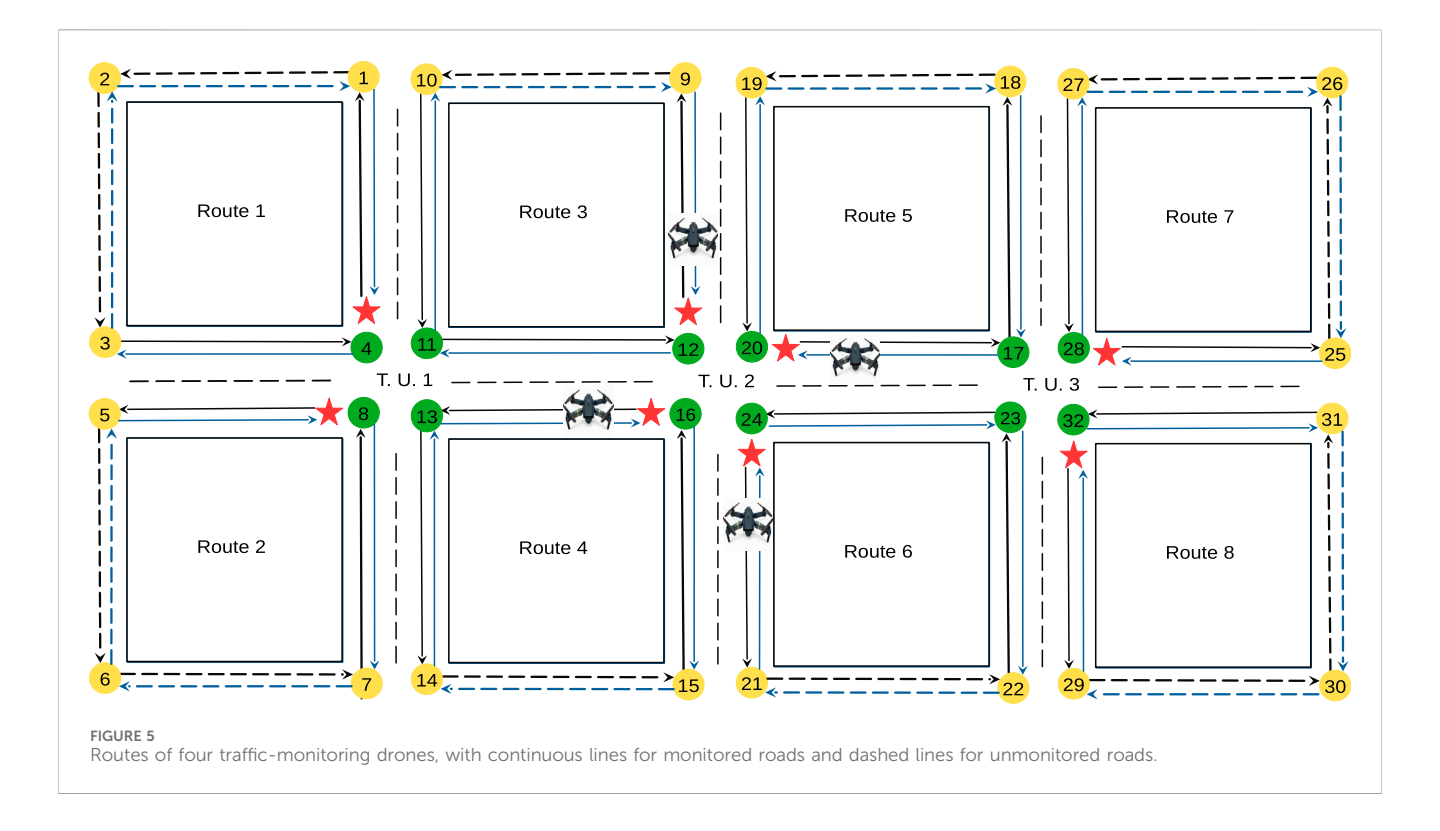
Note that, we do not include the yellow light, since, being a fixed duration signal, generally overlapping with the green—and sometime with the red—light, we consider that it has only marginal and potentially negligible effects on the emergence and dissipation of traffic congestion. Nevertheless, at this stage of our exploration, the elimination of yellow light considerably simplifies our model.



## 2.3 The traffic model

We use the cell transition model (CTM) to simulate the vehicles' movement on the road network (Yao et al., 2022). CTM is a cellular automaton traffic model that is widely used in the literature since it offers several advantages in terms of definition and analysis of traffic dynamics based on cells' input and output flow. The model

represents the road network as a series of discrete cells, in which the length of each cell is calculated based on the distance travelled by free-flow traffic in one evaluation time step. Each cell corresponds to a segment of the road. The non-continuous (in time and space) flow of traffic between adjacent cells of the CTM is shown in Figure 4a, where for cell i,  $\eta_{i(t)}$  refers to the number of vehicles in the cell,  $f_i$  is the incoming traffic flow into the cell and  $f_{i+1}$  the outgoing traffic



flow from the cell. In our road network, there are two sets of four cells between two consecutive intersections as shown in Figure 4b. One sets models all vehicles entering into an intersection (i.e., the vehicles that proceed straight, those turning right, and those turning left at the intersection), and the other sets model the vehicles leaving an intersection (i.e., the vehicles joining the leg while moving forward, those joining the leg after a right turn, and those joining the leg from a left turn). In each set of cells, cell 1 is the furthest, and cell 4 is the closest to the corresponding intersection entry point (see Figure 4b). Hence, the number of vehicles in cell i at time (t+1) is defined as:

$$\eta_i(t+1) = \eta_i(t) + f_i(t) - f_{i+1}(t); \tag{1}$$

$$f_i(t) = q_i(t)\Delta t = \min\{v_f k_{i-1}\Delta t, q_{max}\Delta t - w\Delta t k_i\}$$
 (2)

where,  $\Delta t$  is the sample time, w and  $v_f$  are the reverse wave speed and the free flow speed, respectively, and k is the congestion density. In traffic flow theory, reverse wave speed characterizes how quickly a traffic jam forms and moves in the opposite direction to vehicle travel and free flow speed refers to the velocity at which vehicles move under uncongested traffic conditions.

The following requirements must be met for the traffic flow:

$$\eta_{i-1}(t) = \nu_f k_{i-1} \Delta t \tag{3}$$

$$Q_{i}(t) = q_{max} \Delta t \tag{4}$$

$$\eta_i(t) \le Q \tag{5}$$

with Q the maximum capacity of cell i, and  $q_{max}$  the maximum traffic flow. Therefore, by substituting Equations 3–5 into Equation 2, the number of cars leaving cell i-1 toward cell i can be rewritten as follows:

$$f_{i}(t) = min\{\eta_{i-1}(t), Q_{i}(t), -(v/w_{f})[N_{i}(t) - \eta_{i}(t)]\}$$
 (6)

with  $N_i(t)$  the maximum number of vehicles that can stay at time t in cell i. Two capacity variables  $S_i(t)$  and  $R_i(t)$  are introduced to refer to the number of vehicles that can be sent and received by cell i at time t, with:

$$S_i(t) = min(\eta_i(t), Q_{i+1}(t))$$
 (7)

$$R_i(t) = \min(Q_i(t), -(v/w_f)[N_i(t) - \eta_i(t)]$$
(8)

Based on the Equations 6-8 can be simplified as follows.

$$f_i(t) = min(S_{i-1}(t), R_i(t))$$
 (9)

More detailed information about CTM model can be found in (Yao et al., 2022). Based on Equation 9, CTM is suitable for capturing fundamental traffic dynamics. However, it has limitations in representing more complex behaviours, especially in urban environments with dynamic conditions, such as: frequent lane changes, pedestrian interactions, heterogeneous vehicle movements and/or driving behaviour, etc. These phenomena can be more effectively captured by microscopic traffic flow simulation software, which we will use in future works.

## 2.4 Route planning for drones

Four drones monitor and manage the road traffic on the entire road network by flying along predefined paths. Each drone is assigned to a specific portion of the road network which can be monitored by following two distinctive routes. In each route, only the roads that are part of the monitored road network are considered by the drones, as shown in Figure 5. Each drone keeps on flying on the same route unless specific traffic conditions are met, following which the done swap route (see Section 2.5 for details on the

conditions triggering the route swapping). In the current implementation, drone coordination is managed by the traffic unit at the meeting point, which assigns tasks and ensures each drone collects relevant data. While this centralized approach is sufficient for the three-intersection network, we acknowledge that larger networks would require more sophisticated, possibly decentralized, coordination strategies. The camera is oriented in a nadir (downward-facing) position of the drones with a fixed angle of view. In the cellular model, to ensure complete coverage of a single cell, the drones should fly at a specific flight altitude (h) set as follows:

$$h = \frac{cell_{dimention}}{2.\tan(\theta/2)};$$
(10)

where *h* refers to the flight altitude required by drones to fully cover an area with the cell dimension ( $\mathit{cell}_{\mathit{dimention}}$ );  $\theta$  is the camera's field of view angle (Yang et al., 2024). Based on Equation 10, it is important to highlight that data quality decreased with increasing altitude. Since drones fly at different speeds, it takes different times for them to completely monitor a specific route. While flying above the road, the drones monitor the traffic by counting the number of vehicles in the cell at their current position. Figure 5 shows the four drones and the two routes per drone  $DR_{(i,j)}$ , with  $i \in 1, 2, 3, 4$ referring to the drone, and  $j \in 1, 2$  indicating the route. Moreover, in Figure 5, the black and blue arrows indicate the directions of the drones' movement within each route and the flow of traffic in CTM, respectively. Moreover, the red stars indicate the starting point of each route, the yellow circles mark a road change within the route, and the green circles are the meeting points placed at the intersections. Anytime a drone reaches this point, it communicates to the corresponding traffic light the number of vehicles found in each of the cell traversed during the latest loop on the route. In the current system, the data transmission from drones to traffic units is implemented as a one-way communication at predefined meeting points, which minimizes latency and simplifies synchronization. However, we acknowledge that in larger networks, where continuous or real-time updates are required, communication delays could become a bottleneck. To address this, future extensions may incorporate low-latency communication protocols, time-slot scheduling, or multi-channel communication systems to ensure timely and reliable data exchange between drones and traffic agents. Weather conditions can act as external disturbance for the motion control of drones. Since several studies have already illustrated robust drones motion controller in adverse weather conditions, for the sake of simplicity, we did not consider this element (i.e., wind disturbance) in our model. Finally, drones travel timing between different routes is not considered. Given that such rerouting typically happens faster than signal cycle updates, we consider its impact on timing synchronization to be negligible at least in this first investigation of the system performance.

## 2.5 Traffic signal optimisation

The simultaneous perturbation stochastic approximation (SPSA) algorithm is used to set the conditions to minimise the traffic and to avoid traffic congestion on the road network. The

information about the current traffic conditions (i.e., the number of cars in each of the monitored cells) are communicated at regular intervals by the drones to the closest traffic lights every time they reach a meeting point. The traffic light runs the SPSA algorithm to adjust the duration of the green light with the objective of reducing traffic while taking into account constraints determined by the intersection signal timing control and the flow transmission relationship between cells. The SPSA algorithm is a powerful heuristic method that gradually approximates the optimal solution by iteratively estimating the gradient information of the objective function. The algorithm employs two estimated values of the objective function, which is independent of the dimension of the optimisation problem. The feature of perturbing each variable in both positive and negative directions allows the algorithm to estimate the gradient of the objective function more robustly. After perturbing the parameters, SPSA observes the corresponding changes in the objective function. By averaging these perturbations, SPSA computes an approximation of the gradient, adapting its steps based on this approximation to iteratively refine the solution. This adaptability allows SPSA to handle noisy objective functions and to converge efficiently, even in the presence of uncertainties or fluctuations. In our road traffic scenario, the objective function tries to minimise the overall delay D(t) of all cells in a street. The duration of green light G of each traffic unit is the decision variable to minimise the overall delay. The iteration equation of SPSA is formulated as illustrated in Algorithm 1;

```
Input: \hat{x}_0, a_0, C_0
Output : \hat{x}_{k+1}
Compute (k \text{ Iteration})
1. Defines parameters a_k and C_k:
     a_k = a/(A+k+1)^{\alpha}
     C_k = C/(k+1)^{\gamma}
2. Generate two estimated value:
     L(\hat{x}_k + C_k * \delta_k)
     L(\hat{x}_{k} - C_{k} * \delta_{k})
3. Calculates the approximation gradient:
     \hat{g}(x_k) = L(\hat{x}_k + C_k * \delta_k) - L(\hat{x}_k - C_k * \delta_k) / 2C_k * \delta_k
4. Update:
     \hat{x}_{k+1} = \hat{x}_k - a_k * \hat{g}(x_k)
5. Stop if therequirements
     are reached or end of maximum number of
     iterations, otherwise, k = k + 1 and returns to step 1.
```

Algorithm 1 SPSA.

Where,  $\hat{x}_k$  is the estimated value at the  $k_{th}$  iteration,  $a_k$  represents a scalar gain coefficient,  $\hat{g}(x_k)$  is the estimated value of the gradient  $g(x_k)$ , C is a positive scaler, a,  $\alpha$ , A, and  $\gamma$  are nonnegative coefficients. In order to set the values of the algorithm's parameters, we followed the theoretical recommendations illustrated in (Yao et al., 2022). However, we also empirically tuned these values to enhance the algorithm convergence stability and performance under the conditions set by the traffic dynamics modelled in this study. The mentioned algorithm consists of 5 steps. In the first step, the sequences of  $a_k$  and  $C_k$  generate a p dimensional random vector, which is independently and identically distributed with zero mean. Next step calculates two estimation values of the

objective function. In the third step, asynchronous perturbation approximation gradient of the unknown gradient  $\hat{g}(x_k)$  are generated. Following the update in step 4, the algorithm checks whether the accuracy criterion and maximum iteration limit have been satisfied; if so, the optimal result is returned. More description about SPSA algorithm can be found in (Yao et al., 2022).

The objective function aims to minimise the time vehicles spend waiting or moving slowly in the total length of each lane by increasing the number of cars leaving each lane. The delay of a single cell is described as the difference between the number of vehicles in cell i at time t (see Equation 1 and the number of departing vehicles as in Figure 4a.

$$d_i(t) = \Delta t \left[ n_i(t) - f_{i+1}, \right] \tag{11}$$

where  $\Delta t$  is step time,  $n_i(t)$  is the number of vehicles in cell i at time t and  $f_{i+1}(t)$  is the number of the outgoing vehicles from cell i at time t. The objective function must be designed for the entire of street to analyse the efficiency of the traffic system in terms of congestion of vehicles. Equation 11 is designed for single cell, so the overall delay for all cells is calculated as:

$$D(t) = \sum_{i=1}^{Y} \Delta t \left[ n_i(t) - f_{i+1}(t), \right]$$
 (12)

Y = 4 is the number of CTM sub-cells for each road network. Finally, the objective function is achieved based on Equation 12 as:

$$minD(t) = min \sum_{i=1}^{Y} \Delta t [n_i(t) - f_{i+1}(t),]$$
 (13)

From Equation 13, it can be concluded that when  $n_i(t) = f_{i+1}(t)$  the entities in cell i are being continuously transferred to cell i+1, resulting in an empty state for cell i at the specific time t. Theoretical convergence to a local minimum is established under the assumption that the objective function is continuously differentiable with a Lipschitz continuous gradient. Additionally, the stochastic noise in the gradient approximation arising from simultaneous perturbations is assumed to be zero-mean with bounded variance (Jia et al., 2023) Finally, some of the parameters of this model, like the 4-cell depth, has been set with any reference to real-world scenario. We cannot exclude that a different parametrisation could bear upon the system performance as illustrated in Section 3.

## 2.6 Constraints

Note that, several assumptions are made to simplify the simulation process and allow for a more detailed investigation into specific aspects of the study. As mentioned above, the fixed length yellow light is not considered. The sum of the green light duration for all traffic lights at an intersection  $S_{\{i,IN_{fr},k,green\}}$  and  $S_{\{i,IN_{l},k,green\}}$  where  $k = \{w, e, s, n\}$  is considered as cycle time as follows:

$$C = \sum_{k=n}^{n} S_{\{i,IN_{fr},k,green\}} + S_{\{i,IN_{l},k,green\}}$$
 (14)

The travel time required by drones to change routes is not considered. By neglecting the travel time for route changes, the

simulation focuses more narrowly on specific aspects of drone behaviour, such as counting vehicles and the communication with the traffic unit layer. Finally, we define  $S_{\{i,IN_{fr},k,green\}}min$ ,  $S_{\{i,IN_{fr},k,green\}}max$  as the minimum and maximum parameters of green traffic lights  $L_{i,IN_{fr},k}$ , respectively, and  $S_{\{i,IN_{l},k,green\}}min$ ,  $S_{\{i,IN_{l},k,green\}}max$  for  $L_{i,IN_{l},k}$  green traffic lights by considering Equation 14.

## **3** Results

In this Section, we show the results of a series of tests aimed at evaluating the efficiency and robustness of the traffic monitoring and management system based on the adjustment of the green light duration of traffic signals using the SPSA optimisation control. In the following, we refer to this as the adaptive green light duration condition. In particular, we run three types of tests: i) test A, a test in which a fixed green light duration condition is compared with the adaptive green light duration with traffic data generated by drones monitoring the road network as illustrated in Figure 2. ii) test B, a test in which the adaptive green light duration condition with data generated by a set of fixed camera system is compared with the adaptive green light duration with traffic data generated by drones monitoring the road network; iii) test C, a test in which the adaptive green light duration with data generated by drones monitoring the road network is subjected to a progressively higher volume of traffic entering the road network. In all the three types of tests, the traffic is simulated with the CTM model. The length of each cell of the CTM model is set to 50 m, and the maximum capacity of each cell for the  $L_{i,IN_{fr},k}$  lane is 10 vehicles and for the  $L_{i,IN_{fr},k}$  lane is 5 vehicles, with  $i \in {1,2,3}$  referring to the intersections, and  $k \in W, E, N, S$  referring to the cardinal points. Description and value of parameters are set as shown in Tables 1, 2, respectively.

# 3.1 Test A: comparison between fixed and adaptive green light duration conditions

This is the test in which we compare the development of traffic in a condition in which traffic lights operate with a fixed signalling duration with the development of traffic in a condition in which traffic lights adjust the green light duration with the SPSA optimisation algorithm using data generated dy drones. We assess the system's performance using a constant input flow with 20 vehicles per minute entering  $L_{i,IN_{fr},N}$  and  $L_{i,IN_{fr},S}$  lanes at cell 1, and 10 vehicles per minute entering  $L_{i,IN_l,N}$  and  $L_{i,IN_l,S}$  lanes at cell  $1 \ \forall i \in \{1, 2, 3\}$ . Note that, the inflow of north/south roads is two times more than west/east roads. It is also assumed that, at the beginning of each simulation run, a total number of 20 and 10 vehicles are distributed randomly among the four CTM cells of  $L_{i,IN_{fr},k}$  and  $L_{i,IN_l,k}$ , respectively. We have executed 50 differently seeded simulation runs, differing in the initial distributions of the 20 vehicles among the cells of the  $L_{i,IN_{fr},k}$ . In each simulation run, each traffic light completes 22 full cycles. While during the first 10 cycles, the duration of each green light phase is fixed (i.e., 20 s for phase 1 and 3; 10 s for phase 2 and 4), in the last 12 cycles this duration is set by the SPSA optimisation control to manage traffic as monitored by drones. Note that each simulation run lasts 1,320 s,

TABLE 1 Table of symbols.

Description	Notation	Unit
Intersection	$R_{\{i,j,k\}}$	-
Input Flow	$IN_{fr/l}$	-
Output Flow	$OUT_{fr/l}$	-
Intersection Lane	$L_{\{i,j,k\}}$	-
Traffic Signal	$S_{\{i,j,k,c\}}$	s
Number of Vehicle in Cell	$\eta_{i(t)}$	-
Incoming Flow into Cell i	$f_i$	-
Outgoing Flow from Cell i	$f_{i+1}$	-
Reverse wave speed	ν	km/h
Free flow speed	$w_f$	km/h
Step time	$\Delta t$	s
Simulation duration	T	s
Cycle time	С	s
Drone speed	$S_{\mathrm{Drone}}$	m/s
Max duration of green traffic light for $fr$ lane	$S_{\{i,IN_{fr},k,green\}}max$	s
Min duration of green traffic light for $fr$ lane	$S_{\{i,IN_{fr},k,green\}}min$	s
Max duration of green traffic light for <i>l</i> lane	$S_{\{i,IN_l,k,green\}}max$	s
Min duration of green traffic light for $l$ lane	$S_{\{i,IN_l,k,green\}}$ min	s
Maximum Traffic Flow	$q_{max}$	veh/hr
Flight Altitude of Drone	h	m
Dimension of Cellular Cell	Cell <sub>dimension</sub>	m
Camera Field of View	θ	degree
Drone	$DR_{\{i,j\}}$	-
Objective Function	D(t)	s
Green Light Duration	G	s
Gradient Estimation	$g(x_k)$	-
Positive Scalar	С	-
Positive Coefficients	a, α, Α, γ	-

which is less than the average drone battery life which ranges from approximately 1,200 to 1,800 s, allowing us to model drones' continuous operation without mid-flight stop for battery recharging. To evaluate the performances of the traffic monitoring and management system, we have kept track of the total number of cars in: i)  $L_{i,IN_{fr},W}$  and  $L_{i,IN_{fr},E}$  lanes at the beginning of phase 2 of each traffic light cycle; we refer to this as  $NC - WE_{i,fr}$ , with intersection  $i \in 1, 2, 3$  (see Figure 6a); ii)  $L_{i,IN_{l},W}$  and  $L_{i,IN_{l},E}$  lanes at the beginning of phase 3 of each traffic light cycle; we refer to this as  $NC - WE_{i,l}$ , with intersection i with  $i \in 1, 2, 3$  (see Figure 6b); iii)  $L_{i,IN_{fr},N}$  and  $L_{i,IN_{fr},S}$  lanes at the beginning of phase 4 of each traffic light cycle; we refer to this as  $NC - NS_{i,fr}$ , with intersection i with  $i \in 1, 2, 3$  (see Figure 6c); iv)  $L_{i,IN_{l},N}$  and  $L_{i,IN_{l},S}$  lanes at the beginning of phase 1 of each traffic light cycle; we refer to this as

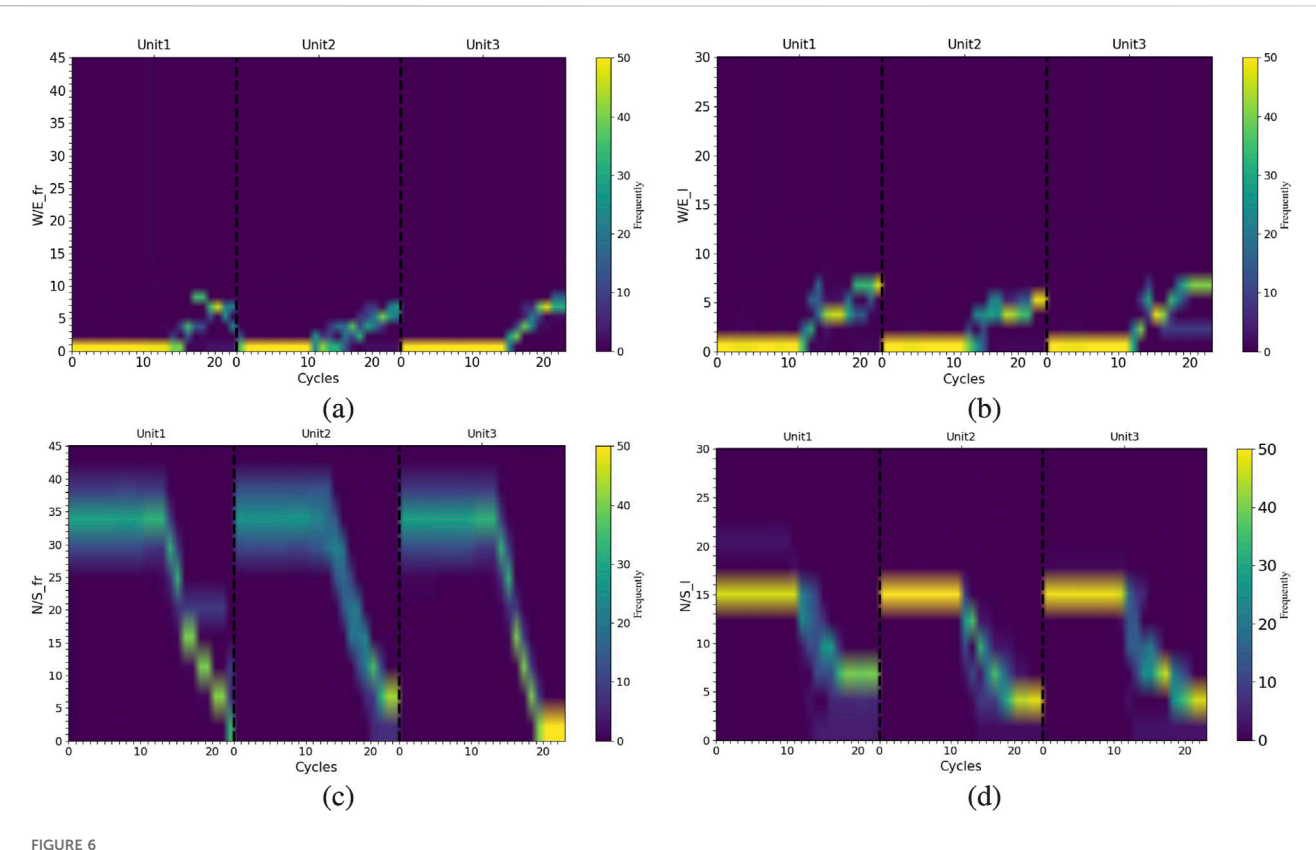
TABLE 2 Values of the simulation parameters used during the evaluation tests.

Parameter	Notation	Value
Reverse wave speed	ν	63 km/h
Free flow speed	$w_f$	60 km/h
Step time	$\Delta t$	2 s
Simulation duration	T	1320 s
Cycle time	С	60 s
Drone speed	$S_{\mathrm{Drone}}$	16 m/s
Max duration of green traffic light for $fr$ lane	$S_{\{i,IN_{fr},k,green\}}max$	26 s
Min duration of green traffic light for $fr$ lane	$S_{\{i,IN_{fr},k,green\}}min$	14 s
Max duration of green traffic light for $l$ lane	$S_{\{i,IN_l,k,green\}}max$	14 s
Min duration of green traffic light for l lane	$S_{\{i,IN_l,k,green\}}min$	6 s

 $NC - NS_{i,l}$ , with intersection i with  $i \in 1, 2, 3$  (see Figure 6d). Note that the traffic light phases at which cars are counted, correspond to points in time that follow the end of the green light for the corresponding lanes. That is, times in which the number of cars is expected to be at its minimum value.

The results of our evaluation tests are shown in Figure 6, where Figures 6a,b refer to the evolution of traffic on the west/east direction, and Figures 6c,d refer to the evolution of traffic on the north/south direction at each intersection i with  $i \in 1, 2, 3$ . If we focus our attention on the evolution of traffic during the first 10 cycles, when the duration of the green light is fixed, we see that, the most frequently observed values for the number of cars in the west/est direction are those close to zero (see the values of NC –  $WE_{i,fr}$  in Figure 6a, and the values of  $NC - WE_{i,l}$  in Figure 6b, from cycle 0-10). This means that at every cycle, the "fixed" duration of the green light in phase 1 and 2 is sufficient to empty the lanes  $L_{i,IN_{fr},W}$ ,  $L_{i,IN_{fr},E}$ ,  $L_{i,IN_{l},W}$ , and  $L_{i,IN_{l},E}$ . Conversely, the most frequently observed values for the number of cars in the north/ south direction are those close to 35 for the vehicles moving forward and turning right (see the values of  $NC - NS_{i,fr}$  in Figure 6c, from cycle 0-10) and 15 for the vehicles turning left (see the values of  $NC - NS_{i,l}$ ) in Figure 6d, from cycle 0–10). This means that at every cycle, the "fixed" duration of the green light in phase 3 and 4 is not sufficient to empty the lanes  $L_{i,IN_{fr},N}$ ,  $L_{i,IN_{fr},S}$ ,  $L_{i,IN_{l},N}$ , and  $L_{i,IN_{l},S}$ . In other words, given the input flow with 20 vehicles per minute entering  $L_{i,IN,N}$  and  $L_{i,IN,S}$  lanes at cell 1, and 10 vehicles per minute entering  $L_{i,IN,W}$  and  $L_{i,IN,E}$  lanes at cell 1  $\forall i \in 1, 2, 3$ , the fixed duration of green light tends to generate traffic on the north/ south directions.

From cycle 10, to the end of the simulation time (i.e., cycle 22), we see that the traffic evolves in a radically different way in response to the activation of the adaptive traffic unit, which by receiving data on traffic from drones, it increases the duration of the green light for phase 3 (i.e.,  $S_{\{2,IN_f,N,green\}}$ ,  $S_{\{2,IN_f,S,green\}}$ ) and phase 4 (i.e.,  $S_{\{2,IN_l,N,green\}}$ ,  $S_{\{2,IN_l,S,green\}}$ ), while reducing the green light duration of phase 1 (i.e.,  $S_{\{2,IN_f,W,green\}}$ ,  $S_{\{2,IN_f,E,green\}}$ ), and phase 2 (i.e.,  $S_{\{2,IN_l,W,green\}}$ , and  $S_{\{2,IN_l,E,green\}}$ ). This effect, starting at cycle 10 until cycle 13, is illustrated in Figure 7, which shows the mean and standard deviation of the duration of the green signal traffic lights



Graphs showing the evolution of traffic monitored by showing the frequency of the different values of (a)  $NC - WE_{i,fr}$ , (b)  $NC - WE_{i,fr}$ , (c)  $NC - NS_{i,fr}$ , and (d)  $NC - NS_{i,fr}$ , for every intersection i with  $i \in 1, 2, 3$ , at every traffic light cycle from cycle 0 to cycle 22. Note that, the optimisation algorithm starts operating at cycle 10 until cycle 22.

over 50 differently seeded simulation runs. This has an immediate effect on traffic as shown in Figure 6. In particular, we observe that from cycle 10 to cycle 22, the most frequently observed values for the number of cars in the north/south direction generate a decreasing trend to about zero for vehicles moving forward and turning right (see the values of  $NC - NS_{i,fr}$  in Figure 6c, from cycle 10–22) and between 4 and 6 for vehicles turning left (see  $NC - NS_{i,l}$  in Figure 6d, from cycle 10-22). This means that the SPSA optimisation algorithm manages to reduce the traffic on the north/south direction in spite of the input flow described above. At the same time, the most frequently observed values for the number of cars in the west/east direction generate a slightly increasing trend that reaches the threshold of 7 vehicles (see the values of  $NC - WS_{i,fr}$  in Figure 6a, and of  $NC - WS_{i,l}$  in Figure 6b, from cycle 10-22). This means that, given that the duration of the traffic light cycle is fixed, the adjustment on the duration of the green light for all phases inevitably causes a slight increase in the traffic on the west/east direction in response to a large decrease in traffic in the north/south direction.

# 3.2 Test B: comparison between camera generated and drones generated traffic data

To provide a comparative framework that helps to assess the performance of the drones-based system, we have compared the

development of traffic in a condition in which traffic lights adjust the green light duration with the SPSA optimisation algorithm using data generated by a fixed set of cameras, with the development of traffic in a condition in which traffic lights adjust the green light duration with the SPSA optimisation algorithm using data generated by drones. In the fixed camera condition, we assume that each intersection is equipped with four stationary cameras each oriented toward a different cardinal point. Each camera has a field of view of 50 m sufficient to correctly count cars in the last cell (i.e., cell 4, the cell in the immediate proximity of the traffic light) of the viewed lanes. Thus, contrary to the drones-based system which delivers data related to the number of cars along the entire flying path, cameras can only generate and deliver accurate data related to the cells closest to the traffic lights. Note that our aim is to model a generic camerabased system that we assume with a limited view of the roads compared to the drones-based system. This assumption follows from general considerations on practical aspects related to the specifications of cameras used for this type of application, as well as on other aspects such as the height at which cameras are usually mounted. This limitation may not necessarily apply to all camerabased systems for traffic monitoring. This issue will be discussed in Section 4.

In the tests, the initial traffic conditions and the frequency of cars entering into the road network as well as any parameters of the system remain unchanged from previous set of tests illustrated in Section 3.1. Moreover, as in tests A, we have executed 50 differently

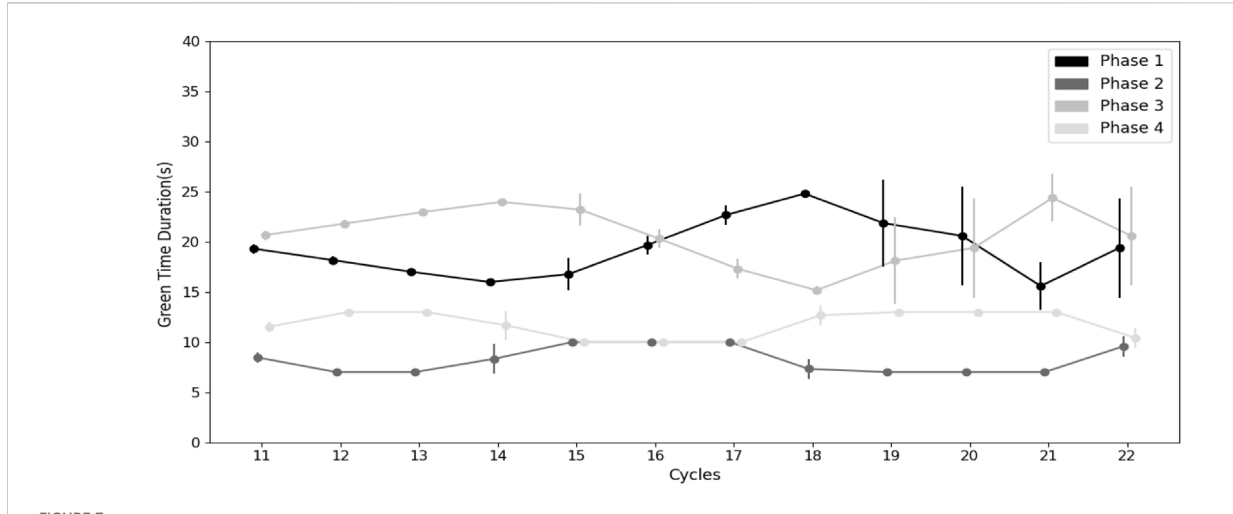


FIGURE 7
Graph showing the mean value and standard deviation, over 50 simulation runs, of the optimised duration of the green signals of traffic light 2, for phase 1 (black line, corresponding to signals  $S_{\{2,IN_b,W,green\}}$ ,  $S_{\{2,IN_b,E,green\}}$ ), phase 2 (dark grey line, corresponding to signals  $S_{\{2,IN_b,W,green\}}$ , and  $S_{\{2,IN_b,E,green\}}$ ), phase 3 (medium grey line, corresponding to signals  $S_{\{2,IN_b,N,green\}}$ ,  $S_{\{2,IN_b,S,green\}}$ ), and phase 4 (light grey line, corresponding to signals  $S_{\{2,IN_b,N,green\}}$ ,  $S_{\{2,IN_b,S,green\}}$ ). Traffic data collected by drones.

seeded simulation runs, differing in the initial distributions of the 20 vehicles among the cells of the  $L_{i,IN_{fr},k}$ . In each simulation run, each traffic light completes 22 full cycles. While during the first 10 cycles, the data for the SPSA optimisation algorithm is generated by fixed cameras, in the last 12 cycles the data for the SPSA optimisation algorithm is generated by drones.

The results of our evaluation tests are shown in Figure 8, where Figures 8a,b refer to the evolution of traffic on the west/east direction, and Figures 8c,d refer to the evolution of traffic on the north/south direction at each intersection i with  $i \in 1, 2, 3$ . At the beginning of the simulation, green lights are assigned to  $L_{i,IN_{fr},W/E}$ lane of each intersection, resulting in a near-zero vehicles at cycle 0 in this lane of each traffic light or unit. This can be clearly seen in Figure 8a, which shows the number of cars at the beginning of phase 2 of each cycle of each traffic light or unit. However, we notice that, while the system operates on cameras the number of cars at each intersection tends to increase until roughly 20 at cycle 10 (see Figure 8a from cycle 0-10). On the contrary, on the  $L_{i,IN_{fr},N/S}$ lane of each intersection, we observe a progressive decrease in the number of cars from cycle 0 to cycle 10. This can be seen from Figure 8c, showing the number of cars at the beginning of phase 4 of each cycle of each traffic light or unit. This indicates that while operating on camera, the traffic management system resolves congestion on the  $L_{i,IN_{fr},N/S}$  lanes while inevitable producing more traffic on the  $L_{i,IN_{fr},W/E}$  lane of each intersection. From cycle 11 to cycle 22, when the traffic management system operates on drones data, we observe an identical trend on traffic that sees cars increasing on the  $L_{i,IN_{fr},W/E}$  lane of each intersection and cars decreasing on the  $L_{i,IN_{fr},N/S}$  lane of each intersection (see Figures 8a,c from cycle 11 to cycle 22). Nevertheless, if we compare the traffic trend generated by camera data (from cycle 0 to cycle 10) with the trend generated by drones data (from cycle 11 to cycle 22), we clearly see that the management system is more effective in managing overall traffic on both  $L_{i,IN_{fr},W/E}$  and  $L_{i,IN_{fr},N/S}$  lanes when operating on drones generated data.

The traffic develops in a similar way on the  $L_{i,IN_l,W/E}$  and  $L_{i,IN_l,N/S}$  lanes of each intersection, with a progressive decrease in traffic on the  $L_{i,IN_l,N/S}$  lane of each intersection (see Figure 8d), and a progressive increase on traffic on the  $L_{i,IN_i,W/E}$  lane of each intersection (see Figure 8b). The management system continues to operate more effectively when data is generated by drones (see Figures 8b,d, from cycle 11 to cycle 22) than when data is generated by cameras (see Figures 8b,d, from cycle 0 to cycle 10). The results shown in Figure 8 indicate that the SPSA algorithm shows limited effectiveness when operated by camera generated data. This happens when the cells monitored by cameras (i.e., the cell in the proximity of the traffic lights) reach full capacity on both  $L_{i,IN_{fr},W/E}$  and  $L_{i,IN_{fr},N/S}$ lanes, or on  $L_{i,IN_l,W/E}$  and  $L_{i,IN_l,N/S}$  lanes. Under this condition the camera-based system, due to its limitations, can not detect any further increase in traffic congestion and the optimization control convert to the fix control strategy as can be seen in Figure 9 after cycle 18. Consequently, it cannot provide sufficiently informative data to the SPSA algorithm to keep on effectively managing traffic.

## 3.3 Test C: adaptive green light duration on a progressively higher volume of traffic

In a further set of post-evaluation tests, we have evaluated the robustness of the SPSA optimisation algorithm to cope with a progressively higher volume of vehicles entering into the road network. In particular, we have considered different scenarios, in which the input flow of vehicles at intersection i = 2 is set in the following: for the north-south direction to input flow is fixed in all scenarios to 40 vehicles with 20 vehicles entering cell 1 of lane  $L_{2,IN,N}$ , 20 vehicles entering cell 1 of lane  $L_{2,IN,S}$ . Conversely, the input flow for the west-east direction increases from 20 to 40 vehicles, with an initial scenario in which 10 vehicles enter cell 1 of lane  $L_{2,IN,W}$ , and 10 vehicles enter cell 1 of lane  $L_{2,IN,E}$ . In each of the following scenarios, the numbers of vehicles entering

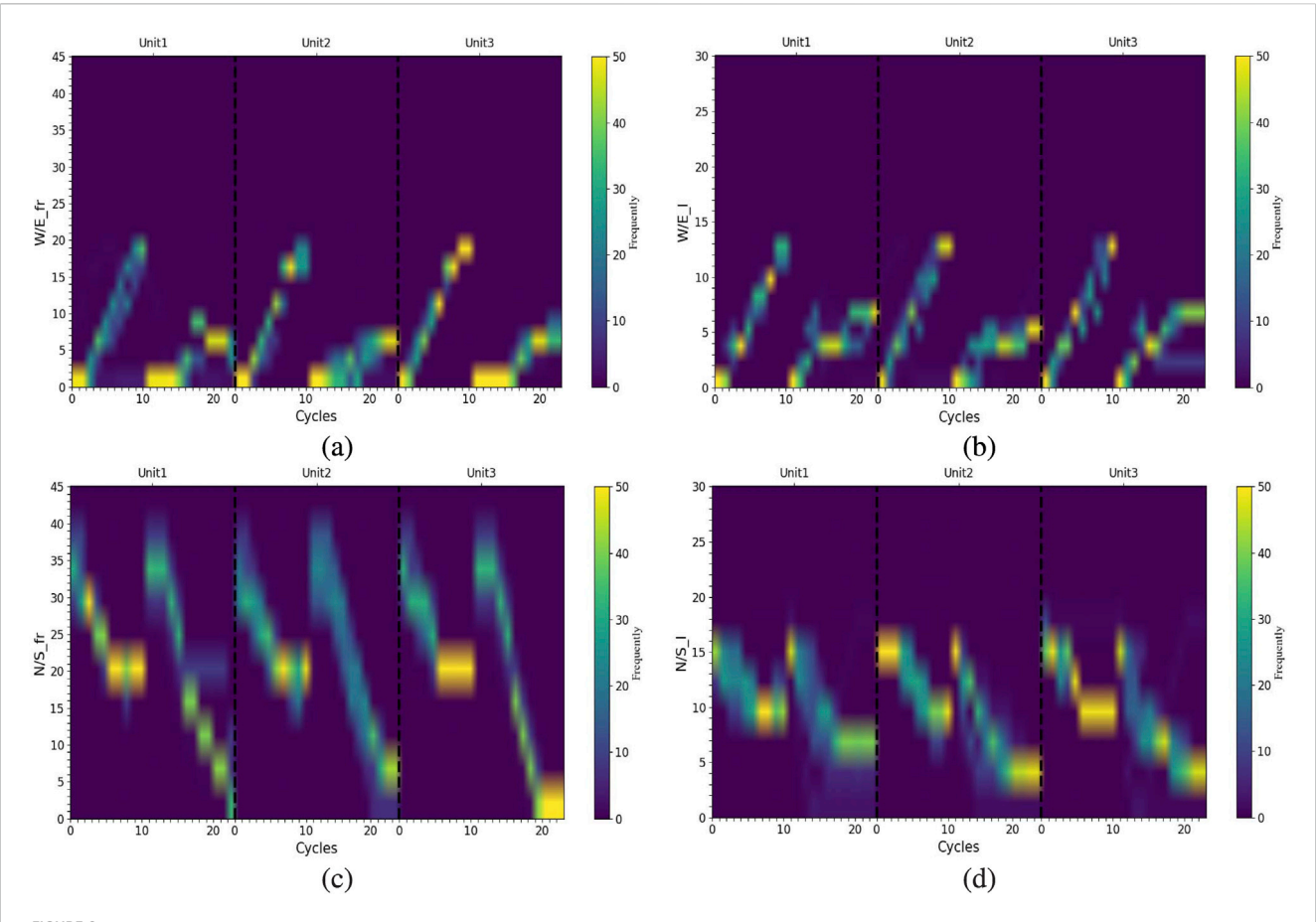
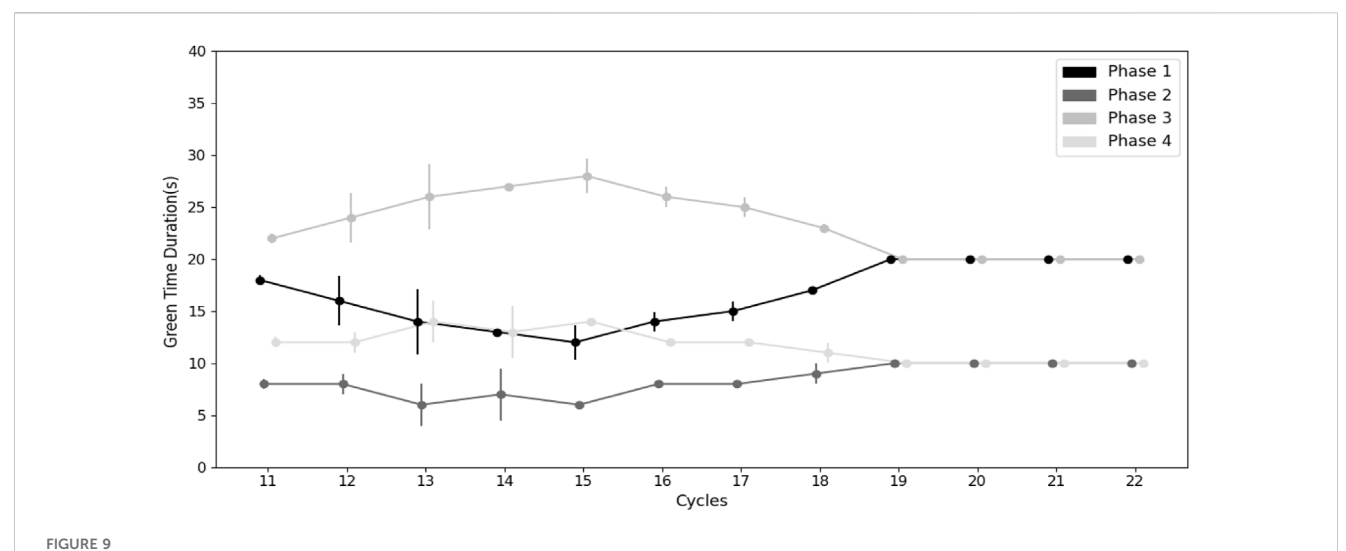


FIGURE 8 Graphs showing the evolution of traffic monitored by showing the frequency of the different values of (a)  $NC - WE_{i,fr}$ , (b)  $NC - WE_{i,fr}$ , (c)  $NC - NS_{i,fr}$ , and (d)  $NC - NS_{i,fr}$ , for every intersection i with  $i \in 1, 2, 3$ , at every traffic light cycle from cycle 0 to cycle 22. The optimization algorithm utilizes data collected from fixed cameras during cycles 0 to 10, and from drones during cycles 10 to 22.

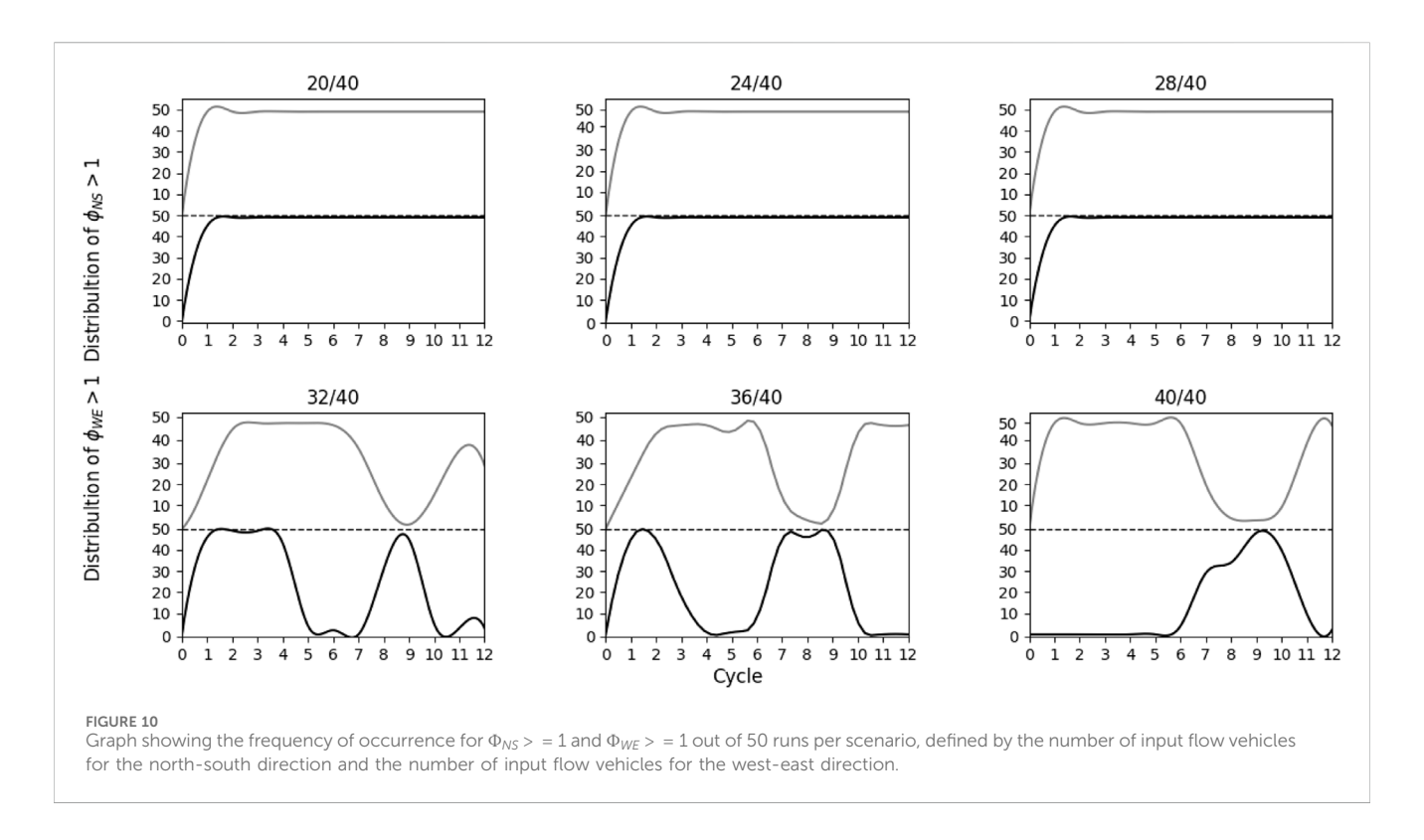
the  $L_{i,IN,W}$  and  $L_{i,IN,E}$  is progressively increased by 2 vehicles until to the point at which the input flow of vehicles is the same for both directions (i.e., 40 vehicles north-south and 40 west-east). This gives rise to the following 6 scenarios: 40/20, 40/24, 40/28, 40/32, 40/36, 40/40, in which the first number refers to the vehicles entering the north-south direction and the second number those entering the west-east direction. In each scenario, at time 0 of each simulation run there are 30 randomly positioned vehicles among the road cells. For each scenario, we run 50 differently seeded runs in which we vary the initial position of these 30 vehicles. During these tests, we computed: i)  $\Phi_{NS}$  as the fraction of the number of vehicles leaving lanes  $L_{i,IN_{fr},N}$ ,  $L_{i,IN_{l},N}$ ,  $L_{i,IN_{fr},S}$ ,  $L_{i,IN_{l},S}$ , to the total number of vehicles entering the north-south direction; ii)  $\Phi_{WE}$  as the fraction of the number of vehicles leaving lanes  $L_{i,IN_{fr},W}$ ,  $L_{i,IN_{l},W}$ ,  $L_{i,IN_{fr},E}$ ,  $L_{i,IN_{l},E}$ , to the total number of vehicles entering the northsouth direction.

Figure 10 shows the results of the robustness test by illustrating, for each scenario, and for each traffic light cycle, the frequency occurrence for  $\Phi_{NS} > = 1$  and  $\Phi_{WE} > = 1$  out of 50 runs per scenario. When these two metrics are bigger than 1, it means that the vehicles exiting are more than the vehicles entering the

respective lanes, with a relatively fluid traffic flow. Additionally, when the number of vehicles exiting equals the number of vehicles entering, traffic conditions remain stable, preventing the occurrence of traffic jams. Conversely, when these two metrics are not bigger than 1, this is a sign that the traffic is increasing. The graph in Figure 10 clearly shows that, for scenarios 40/20, 40/24, 40/28, the traffic management system manages to keep the traffic fluid by adjusting the green light duration of the traffic light at intersection 2. For scenario, 40/32, 40/36, 40/40 the traffic management system progressively lose effectiveness with a clear increase of volume of traffic indicated by the decrease of the frequency of occurrence for  $\Phi_{NS} > 1$  and  $\Phi_{WE} > 1$ . It is interesting to notice that, beyond scenario 40/28, the traffic management system realises that the traffic is increasing in both directions (north-south and west-east). Thus, it tries to reduce the traffic first in one direction and then in the other one. However, since that the duration of the traffic light cycle is fixed, the actions aimed at mitigating the traffic in one direction tend to produce the opposite effect on the other direction. Given the progressively high input flow of vehicles, the system is not capable of re-establishing a fluid traffic condition in both directions.



Graph showing the mean value and standard deviation, over 50 simulation runs, of the optimised duration of the green signals of traffic light 2, for phase 1 (black line, corresponding to signals  $S_{\{2,IN_R,W,green\}}$ ,  $S_{\{2,IN_R,E,green\}}$ ), phase 2 (dark grey line, corresponding to signals  $S_{\{2,IN_R,W,green\}}$ , and  $S_{\{2,IN_R,E,green\}}$ ), phase 3 (medium grey line, corresponding to signals  $S_{\{2,IN_R,N,green\}}$ ,  $S_{\{2,IN_R,S,green\}}$ ), and phase 4 (light grey line, corresponding to signals  $S_{\{2,IN_R,N,green\}}$ ,  $S_{\{2,IN_R,S,green\}}$ ). Traffic data collected by fixed camera.



## 4 Conclusion

This paper describes and evaluates a simulated drones-based system for traffic surveillance and management. In our model, the drones patrol different parts of the road network by counting cars forming the urban traffic. The number of cars are communicated by drones to traffic lights, which, by running the SPSA optimisation

algorithm, adapt the green light duration to resolve any eventual congestion. In our study, the road network is composed of eight roads and three signalled intersections. The roads are patrolled by four drones deployed to monitor the road traffic by flying along predefined paths. We have evaluated the drones-based system by monitoring the traffic on the road network under two different conditions: with fixed (predefined green light duration) and with

adaptive (i.e., SPSA determined) green light duration. We have also compared the drones-based system with a sensor-network based surveillance system made of cameras placed at the road intersections pointing to the four different legs of each signalled intersection. Compared to the drones-based system, the sensor-network based system is conceived limited in its capacity to count cars, since the cameras precisely count cars only in the proximity of traffic lights1. The evaluations are run under specific initial traffic conditions and predefined number of cars entering the road network with more cars entering the N/S than the W/E lanes. We show that with the fixed light duration, the number of cars on the N/S lanes (i.e., the most congested lanes) remains constant with cars jammed entire the roads at each intersection. With the adaptive green light duration, the number of cars on the N/S lanes tends to progressively decrease until no cars jammed entire the roads at each intersection. This is the result of the effects of the SPSA optimisation algorithm which increases the green light duration for the N/S lanes in response to data generated by drones. Since the increase of the green light duration for the N/S lanes corresponds to a decrease of the green light duration for the W/E lanes, the number of cars on these lanes tends to slightly increase. In summary, we have shown that, contrary to the fixed green light duration condition, the adaptive green light duration condition is effective in resolving traffic congestion determined by the flux of incoming cars into the network. The comparison between the drones-based and the sensor-network based system demonstrates that the drones-based system is more effective than the sensor-network based system in resolving traffic congestion.

We acknowledge that, as a first model evaluating a specific urban traffic monitoring and management system based on drones counting cars and optimised system adjusting green light duration, several simplification have been made. On top of those already discussed in 2.6, in our model we assume that four drones are sufficient to exhaustively patrol the entire road network. This may not necessarily be the case especially in large cities, where a too high number of drones may be required to exhaustively patrol the road network. In this study, we do not look at phenomena related to the ratio between number of drones and extension of the road network. Nevertheless, these issues may be of absolute relevance for a system where traffic is monitored by drones and managed by an optimisation algorithm working on drones generated data. If the road network is too large to be exhaustively patrolled by the available drones, several issues emerge related to the capability of drones: i) to position themselves in order to maximise traffic observability; ii) to redeploy themselves in response to changes in the traffic conditions; iii) to manage energy efficiently to maximise batterylife and operation time. Moreover, in this study we do not consider the possibility of replacing drones once their batteries are exhausted to monitor and manage traffic for a period of time longer than the average drone battery life. This can be achieved by creating one or more charging points where drones can return and autonomously recharge their batteries. Given that drones have the capacity to take off and to land vertically, charging points could be created in urban environment by exploiting already existing facilities, such as flat roofs of sufficiently high buildings. We acknowledge that a time complexity/ computational cost analysis of the drone-based system is required to correctly evaluate and effectively tackle some of the above mentioned issues which significantly impact on the possibility to deploy this system in real-world conditions. We leave this analysis to future work.

Another aspects which we did not consider is related to the synchronisation of traffic lights behaviour. Clearly, a system in which traffic lights located on the same road behave in a synchronous way may be potentially more effective in resolving traffic congestion than a system like the one we modelled in which traffic lights do not interact. The synchronisation or any other form of coordination between traffic lights can not be achieved by the system we described in this paper, since there is no means for traffic lights to interact and coordinate. This is another important issue that we intend to explore in future work.

In this study we have compared the drones-based system with a sensor-network based system intentionally conceived limited in its capacity to monitor the road network. Future work may focus on progressively reducing the limitations imposed to the sensor-network based system to quantitatively evaluate the extend to which observability related issues influence the effectiveness of the algorithms adapting the green light duration. This will also be the subject of future work. Finally, it is worth to consider that the use of drones in scenarios like the one illustrated in this paper may require modifications to the current regulations that governed drones operations in terms of both operational and technical requirements.

## Data availability statement

The raw data supporting the conclusions of this article will be made available by the authors, without undue reservation.

## **Author contributions**

DA: Writing – review and editing, Writing – original draft. ET: Writing – review and editing, Writing – original draft.

## **Funding**

The author(s) declare that financial support was received for the research and/or publication of this article. This work was supported by University of Namur.

## Acknowledgments

We would like to express our deepest gratitude to Alexandre Mauroy and Julien Pietquin, for their invaluable guidance, support, and expertise throughout this research. Their insightful feedback

<sup>1</sup> We acknowledge that the camera system could be improved by using as multi-angle camera setups or advanced image processing algorithms. Nevertheless, increasing the number of cameras or introducing multi-angle setups inevitably increases the complexity of deployment and maintenance operations. Such system complexity/cost which progressively increases with the size of the monitored urban areas, may become quickly unsustainable.

and encouragement significantly contributed to the development and completion of this study.

## Conflict of interest

The authors declare that the research was conducted in the absence of any commercial or financial relationships that could be construed as a potential conflict of interest.

## Generative Al statement

The author(s) declare that no Generative AI was used in the creation of this manuscript.

## References

Abdoos, M., and Bazzan, A. (2021). Hierarchical traffic signal optimization using reinforcement learning and traffic prediction with long-short term memory. *Expert Syst. Appl.* 171, 114580. doi:10.1016/j.eswa.2021.114580

Aloqaily, M., Bouachir, O., Al Ridhawi, I., and Tzes, A. (2022). An adaptive uav positioning model for sustainable smart transportation. *Sustain. Cities Soc.* 78, 103617. doi:10.1016/j.scs.2021.103617

Anjum, M. S., Ali, S. M., Subhani, M. A., Anwar, M. N., Nizami, A. S., Ashraf, U., et al. (2021). An emerged challenge of air pollution and ever-increasing particulate matter in Pakistan: a critical reviewe. *J. Hazard. Mater.* 402, 123943. doi:10.1016/j.jhazmat.2020. 123943

Appiah, O., Quayson, E., and Opoku, E. (2020). Ultrasonic sensor-based traffic information acquisition system: a cheaper alternative for its application in developing countries. *Sci. Afr.* 9, e00487. doi:10.1016/j.sciaf.2020.e00487

Atta, A., Abbas, S., Khan, M. A., Ahmed, G., and Farooq, U. (2020). An adaptive approach: smart traffic congestion control system. *J. King Saud University-Computer Inf. Sci.* 32, 1012–1019. doi:10.1016/j.jksuci.2018.10.011

Bisio, I., Garibotto, C., Haleem, H., Lavagetto, F., and Sciarrone, A. (2022). A systematic review of drone-based road traffic monitoring system. *IEEE Access* 10, 101537–101555. doi:10.1109/access.2022.3207282

Causa, F., and Fasano, G. (2021). Multiple uavs trajectory generation and waypoint assignment in urban environment based on dop maps. *Aerosp. Sci. Technol.* 110, 106507. doi:10.1016/j.ast.2021.106507

Chow, A. H., Sha, R., and Li, S. (2020). Centralised and decentralised signal timing optimisation approaches for network traffic control. *Transp. Res. Part C Emerg. Technol.* 113, 108–123. doi:10.1016/j.trc.2019.05.007

Christodoulou, C., and Kolios, P. (2020). "Optimized tour planning for drone-based urban traffic monitoring," in 2020 IEEE 91st vehicular technology conference (VTC2020-Spring) (IEEE), 1–5.

Desmira, D., Abi Hamid, M., Bakar, N. A., Nurtanto, M., and Sunardi, S. (2022). A smart traffic light using a microcontroller based on the fuzzy logic. *IAES Int. J. Artif. Intell.* 11, 809. doi:10.11591/ijai.v11.i3.pp809-818

Dilshad, N., Hwang, J., Song, J., and Sung, N. (2020). "Applications and challenges in video surveillance via drone: a brief survey," in *International conference on information and communication technology convergence (ICTC)*, 728–732.

Elloumi, M., Dhaou, R., Escrig, B., Idoudi, H., and Saidane, L. A. (2018). "Monitoring road traffic with a uav-based system," in 2018 IEEE wireless Communications and networking conference (WCNC) (*IEEE*), 1–6. doi:10.1109/WCNC.2018.8377334

Fadda, M., Anedda, M., Girau, R., Pau, G., and Giusto, D. D. (2022). A social internet of things smart city solution for traffic and pollution monitoring in cagliari. *IEEE Internet Things J.* 10, 2373–2390. doi:10.1109/jiot.2022.3211093

Garcia-Aunon, P., Roldán, J. J., and Barrientos, A. (2019). Monitoring traffic in future cities with aerial swarms: developing and optimizing a behavior-based surveillance algorithm. *Cognitive Syst. Res.* 54, 273–286. doi:10.1016/j.cogsys.2018.10.031

Goetz, A. R. (2019). Transport challenges in rapidly growing cities: is there a magic bullet? *Transp. Rev.* 39, 701–705. doi:10.1080/01441647.2019.1654201

Gohari, A., Ahmad, A. B., Rahim, R. B. A., Supa'at, A. S. M., Abd Razak, S., and Gismalla, M. S. M. (2022). Involvement of surveillance drones in smart cities: a systematic review. *IEEE Access* 10, 56611–56628. doi:10.1109/access.2022.3177904

Guirado, R., Padró, J. C., Zoroa, A., Olivert, J., Bukva, A., and Cavestany, P. (2021). Stratotrans: unmanned aerial system (uas) 4g communication framework applied on the

Any alternative text (alt text) provided alongside figures in this article has been generated by Frontiers with the support of artificial intelligence and reasonable efforts have been made to ensure accuracy, including review by the authors wherever possible. If you identify any issues, please contact us.

## Publisher's note

All claims expressed in this article are solely those of the authors and do not necessarily represent those of their affiliated organizations, or those of the publisher, the editors and the reviewers. Any product that may be evaluated in this article, or claim that may be made by its manufacturer, is not guaranteed or endorsed by the publisher.

monitoring of road traffic and linear infrastructure. Drones 5, 10. doi:10.3390/drones5010010

Hanzla, M., Ali, S., and Jalal, A. (2024). "Smart traffic monitoring through drone images via yolov5 and kalman filter," in 2024 5th international conference on advancements in computational sciences (ICACS), 1–8.

Hassija, V., Chamola, V., Agrawal, A., Goyal, A., Luong, N. C., Niyato, D., et al. (2021). Fast, reliable, and secure drone communication: a comprehensive survey. *IEEE Commun. Surv. & Tutorials* 23, 2802–2832. doi:10.1109/COMST.2021.3084090

Ivancic, W. D., Kerczewski, R. J., Murawski, R. W., Matheou, K., and Downey, A. N. (2019). "Flying drones beyond visual line of sight using 4g lte: issues and concerns," in 2019 integrated communications, navigation and surveillance conference (ICNS) (Herndon, VA, USA), 1–13. doi:10.1109/ICNSURV.2019.8735246

Jia, Z., Wei, Z., and Spall, J. C. (2023). Switch updating in spsa algorithm for stochastic optimization with inequality constraints. *arXiv Prepr. arXiv*. doi:10.48550/arXiv.2302. 02536

Kuang, L., Zheng, J., Li, K., and Gao, H. (2021). Intelligent traffic signal control based on reinforcement learning with state reduction for smart cities. *IEEE Trans. Intelligent Transp. Syst.* 21, 1–24. doi:10.1145/3418682

Kumar, A., Yadav, A. S., Gill, S. S., Pervaiz, H., Ni, Q., and Buyya, R. (2022). A secure drone-to-drone communication and software defined drone network-enabled traffic monitoring system. *Simul. Model. Pract. Theory* 120, 102621. doi:10.1016/j.simpat.2022. 102621

Narisetty, C., Hino, T., Huang, M.-F., Ueda, R., Sakurai, H., Tanaka, A., et al. (2021). Overcoming challenges of distributed fiber-optic sensing for highway traffic monitoring. *Transp. Res. Rec.* 2675, 233–242. doi:10.1177/0361198120960134

Neelakandan, S. B., Berlin, M. A., Tripathi, S., Devi, V. B., Bhardwaj, I., and Arulkumar, N. (2021). Iot-based traffic prediction and traffic signal control system for smart city. *Soft Comput.* 25, 12241–12248. doi:10.1007/s00500-021-05896-x

Nguyen, D. D., Rohacs, J., and Rohacs, D. (2021). Autonomous flight trajectory control system for drones in smart city traffic management. *ISPRS Int. J. Geo-Information* 10, 338. doi:10.3390/ijgi10050338

Qin, Y., Luo, Q., and Xiao, T. (2024). Capacity modeling for mixed traffic with connected automated vehicles on minor roads at priority intersections. *Transp. Plan. Technol.* 1–25. doi:10.1080/03081060.2024.2428410

Radivojević, M., Tanasković, M., and Stević, Z. (2021). The adaptive algorithm of a four-way intersection regulated by traffic lights with four phases within a cycle. *Expert Syst. Appl.* 166, 114073. doi:10.1016/j.eswa.2020.114073

Ravish, R., and Swamy, S. R. (2021). Intelligent traffic management: a review of challenges, solutions, and future perspectives. *Transp. Telecommun. J.* 22, 163–182. doi:10.2478/ttj-2021-0013

Roldán-Gómez, J., Garcia-Aunon, P., Mazariegos, P., and Barrientos, A. (2022). Swarmcity project: monitoring traffic, pedestrians, climate, and pollution with an aerial robotic swarm: data collection and fusion in a smart city, and its representation using virtual reality. *Personal Ubiquitous Comput.*, 1–17doi. doi:10.1007/s00779-022-01662-w

Saleem, M., Abbas, S., Ghazal, T. M., Khan, M. A., Sahawneh, N., and Ahmad, M. (2022). Smart cities: fusion-based intelligent traffic congestion control system for vehicular networks using machine learning techniques. *Egypt. Inf. J.* 23, 417–426. doi:10.1016/j.eij.2022.03.003

Tan, Y., Prasetyo, A. R., Putra, D. D., Wismiana, E., Gunawan, R., and Munir, A. 2020). "Iot-based sensor system for stop line traffic area using

atmega2560 microcontroller," in 14th international conference on telecommunication systems, services, and applications (TSSA 2020) (IEEE), 1–4. doi:10.1109/TSSA51478. 2020.9314061

Tasgaonkar, P. P., Garg, R. D., and Garg, P. K. (2020). Vehicle detection and traffic estimation with sensors technologies for intelligent transportation systems. *Sens. Imaging* 21, 29–28. doi:10.1007/s11220-020-00295-2

Yadav, A., Goel, S., Lohani, B., and Singh, S. (2021). A uav traffic management system for India: requirement and preliminary analysis. *J. Indian Soc. Remote Sens.* 49, 515–525. doi:10.1007/s12524-020-01226-0

Yang, Z., Yang, Y., He, X., and Qi, W. (2024). Incremental coverage path planning method for uav ground mapping in unknown area. *Int. J. Micro Air Veh.* 16, 17568293241262323. doi:10.1177/17568293241262323

Yao, Z., Jin, Y., Jiang, H., Hu, L., and Jiang, Y. (2022). Ctm-based traffic signal optimization of mixed traffic flow with connected automated vehicles and human-driven vehicles. *Phys. A Stat. Mech. Its Appl.* 603, 127708. doi:10.1016/j.physa.2022. 127708

Zhang, R., Ishikawa, A., Wang, W., Striner, B., and Tonguz, O. K. (2020). Using reinforcement learning with partial vehicle detection for intelligent traffic signal control. *IEEE Trans. Veh. Technol.* 22, 404–415. doi:10.1109/tits. 2019.2958859

Zhu, J., Sun, K., Jia, S., Li, Q., Hou, X., Lin, W., et al. (2018). Urban traffic density estimation based on ultrahigh-resolution uav video and deep neural network. *IEEE J. Sel. Top. Appl. Earth Observations Remote Sens.* 11, 4968–4981. doi:10.1109/jstars. 2018.2879368